

Center for Astrophysics Optical Infrared Science Archive I. FAST Spectrograph

JESSICA MINK,¹ WARREN R. BROWN,¹ IGOR V. CHILINGARIAN,^{1,2} DANIEL FABRICANT,¹ MICHAEL J. KURTZ,¹
SEAN MORAN,¹ JAEHYON RHEE,¹ SUSAN TOKARZ,¹ AND WILLIAM F. WYATT¹

¹*Smithsonian Astrophysical Observatory, 60 Garden St., Cambridge, MA 02138, USA*

²*Sternberg Astronomical Institute, M.V. Lomonosov Moscow State University, Universitetsky prospect 13, Moscow, 119234, Russia*

ABSTRACT

We announce the public release of 141,531 moderate-dispersion optical spectra of 72,247 objects acquired over the past 25 years with the FAST Spectrograph on the Fred L. Whipple Observatory 1.5-meter Tillinghast telescope. We describe the data acquisition and processing so that scientists can understand the spectra. We highlight some of the largest FAST survey programs, and make recommendations for use. The spectra have been placed in a Virtual Observatory accessible archive and are ready for download.

Keywords: methods: observational — methods: data analysis — techniques: spectroscopic — astronomical databases: miscellaneous

1. INTRODUCTION

The FAsT Spectrograph for the Tillenghast Telescope (FAST) (Fabricant et al. 1998) is the workhorse moderate-dispersion spectrograph on the Fred L. Whipple Observatory (FLWO) 1.5m Tillinghast telescope, located on Mt. Hopkins, Arizona. Astronomers at the Center for Astrophysics | Harvard & Smithsonian (hereafter CfA) have used FAST to obtain over 160,000 spectra since it began operation in 1994 January. Built to continue work on the CfA Redshift Survey (Geller & Huchra 1989), FAST has taken spectra for the Updated Zwicky Catalog (Falco et al. 1999) and the northern part of the 2MASS Redshift Survey (Huchra et al. 2012), classified thousands of supernovae (Matheson et al. 2008; Blondin et al. 2012; Hicken et al. 2017), monitored symbiotic stars (Kenyon & Garcia 2016) and active galactic nuclei (Trichas et al. 2012), and acquired data for hundreds of other scientific programs.

The goal of this paper is to enable users to understand FAST spectra in order to use the reduced data archive. The Optical Infrared (OIR) Telescope Data Center at the Smithsonian Astrophysical Observatory (SAO) has processed, archived, and distributed over 160,000 raw FAST spectra in the last 25 years.

A Virtual Observatory-accessible archive of reduced FAST spectra is available at the CfA Optical/Infrared Science Archive <http://oirsa.cfa.harvard.edu>. The reduced FAST spectra archive has a number of strengths that include stable spectrograph operations, calibrations, and data processing over the past quarter century. However, the FAST archive is not a uniform set of survey data, and so it is important to understand the data before using it.

We begin with a brief description of the FAST spectrograph and the observing protocols used to acquire raw data. We then discuss the data reduction pipeline used to extract one-dimensional spectra, and the cross-correlation analysis used to derive radial velocities. We present example spectra, and highlight the largest data sets in the FAST archive. We close by describing how to access the data and recommend data quality flags. All of the spectra are stored in standard FITS files. We document the cross-correlation templates used to estimate radial velocities in Appendix B and the full list of the keywords stored in each FITS image header in Appendix C.

2. THE SPECTROGRAPH

FAST is a long-slit optical spectrograph described in detail by Fabricant et al. (1998). Figure 1 presents a schematic of the instrument. Light from the telescope enters from above and is focused onto the slit plate, where a slit-viewing camera enables the observer to align an astronomical target onto the slit. Light that passes

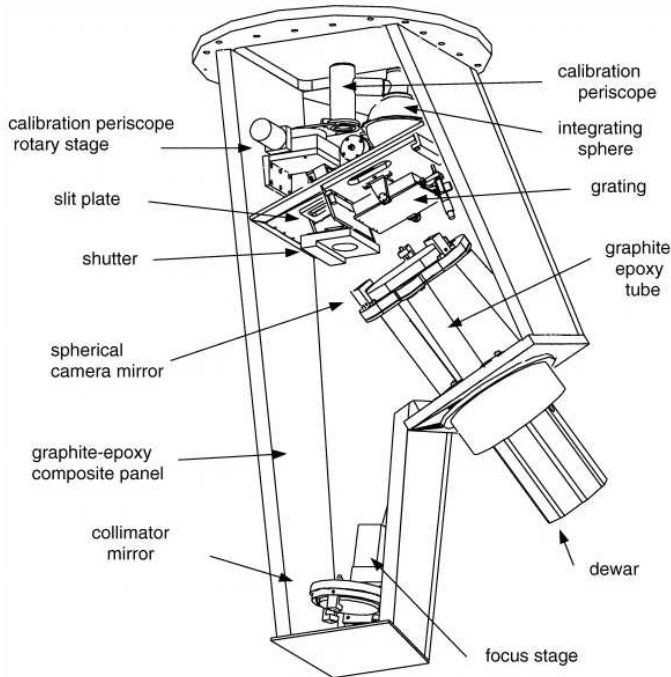


Figure 1. Schematic of the FAST spectrograph. Light enters from the top, passes through the slit plate, reflects off of the collimator mirror at the bottom, is dispersed by a reflection grating, and then is imaged by a folded Schmidt camera onto a CCD detector. The CCD dewar extends to the bottom right. Adapted from Fabricant et al. (1998).

through the slit is reflected off a collimator mirror, is dispersed by a reflection grating, and then is imaged by a folded Schmidt camera onto a CCD detector. An integrating sphere with an incandescent and a helium-neon-argon lamp can be used to illuminate the slit for flat-field and wavelength calibrations, respectively.

2.1. Configurations

The spectrograph is used in different configurations defined by the choice of grating, the grating tilt angle, and slit size. A fourth spectrograph setting, detector binning, defines the sampling in the spatial direction. These settings are recorded in the FITS headers as DISPERSE, TILTPOS, APERTURE, and BIN, respectively.

- FAST has three reflection gratings: a 300 line mm^{-1} and a 600 line mm^{-1} grating blazed at 4750 Å, plus a 1200 line mm^{-1} grating blazed at 5700 Å. Blocking filters are available but in practice never used, with the exception of settings centered around H_α using the 1200 line mm^{-1} grating. Second-order light is thus present above ~ 6500 Å in most spectra.

Table 1. Top Four FAST Configurations^a

Grating (l mm^{-1})	Tilt (mil)	Slit ($''$)	Coverage (Å)	Res. (Å)	%
300	590	3.0	3475—7415	7.2	81%
600	445	1.5	3540—5530	1.8	13%
600	752	2.0	5570—7570	2.3	2%
1200	850	2.0	6200—7200	1.1	1%

^aOrdered by percentage of spectra obtained from 2006 June through 2019 December.

- Central wavelength is controlled by the grating tilt angle. A micrometer, with units of thousandths of an inch, is used to set the tilt angle. Linear equations relate the micrometer value to the approximate central wavelength for each grating, provided in Appendix A. In the FITS headers, starting wavelength is recorded as CRVAL1 and the pixel scale (\AA pix^{-1}) is recorded as CD1_1.
- FAST has five slits with widths of 1.1, 1.5, 2.0, 3.0, and 5.0 arcsec. All slits are 3 arcmin long in the spatial direction. Galaxy and supernova spectra are normally obtained with the 3.0 arcsec slit; stellar spectra are normally obtained with the 1.5 or 2.0 arcsec slits, better matched to typical seeing. Table 1 summarizes spectral coverage and spectral resolution for the four most common configurations, ordered by the percentage of spectra obtained between 2006 June 2006 and 2019 December. Most spectra are acquired with the 300 line mm^{-1} grating, the 3.0 arcsec wide slit, and $2\times$ binning in the spatial direction, a configuration that provides 3475 - 7415 Å spectral coverage at 7.2 Å resolution.
- Since 2006 June, FAST’s detector has been a backside-illuminated, 2688x512 UA STA520A #4377 CCD with a blue-enhanced antireflection coating and $15\ \mu\text{m}$ pixels. This detector, labeled DETECTOR=‘FAST3’ in the fits header, has a dark current of less than 1 electron $\text{hr}^{-1}\ \text{pix}^{-1}$. Earlier-generation CCDs had higher dark current and more defects, but identical pixel scale. All of the thinned detectors exhibit mild 2-3% amplitude fringing in the red end of the spectrum at >6300 Å. The spatial scale is always 0.57 arcsec pix^{-1} along the slit. However, spectra are normally acquired with $2\times$ or $4\times$ binning along the spatial dimension. We tabulate the details of the

Table 2. FAST Detectors

Name	Start Date	End Date	Chip Size	Nspec
CCD	1994-01-08	1994-07-18	2688x512 Loral 51222688 not thinned	3897
FAST1	1994-09-03	1998-04-18	2720x512 thinned	28864
FAST2	1998-04-19	2006-06-19	2720x512 thinned	60699
FAST3	2006-06-20	2019-12-22	2688x512 thinned	48041

CCDs that have been used in Table 2. While CCD dimensions have varied, all have had $15\mu\text{m}$ square pixels. The last column indicates the number of processed spectra in the archive obtained with that detector.

2.2. Throughput

The FAST spectrograph is characterized by high throughput. What matters for the data is total system throughput: the product of the telescope mirrors and the spectrograph optics, grating, and CCD. The total system throughput varies by a factor of 2 or more depending on the state of the optics, but typically peaks around 35% after primary mirror re-aluminization.

Figure 2 plots the total system throughput measured from flux standards observed through a 5 arcsec slit (to minimize slit losses) at airmass < 1.04 on 2014 October 16. The blue line is measured from a hot star, BD+284211, and the red line is measured from a cool star, HD192281. The overall shape of the curves is governed by the blaze function of the 300 line mm^{-1} grating. The low-amplitude oscillations along the curves are real and come from the LLNL Durable Silver coating on the spectrograph collimator and camera mirrors. The divergence at the red end of the spectrum comes from second-order blue (i.e. 3500 \AA) light constructively interfering at first-order red wavelengths (i.e. at 7000 \AA).

Figure 3 plots relative throughput versus time measured from the flux of BD+284211 in two wavelength bands, centered at 3800 \AA and 5600 \AA , normalized to the mean of 25 years of observations. BD+284211 was observed thousands of times in the standard 3 arcsec slit configuration, but not always in photometric conditions. The upper envelope of points in Figure 3 thus provides a measure of relative throughput; the low points are meaningless, due to clouds, bad pointing, and other factors.

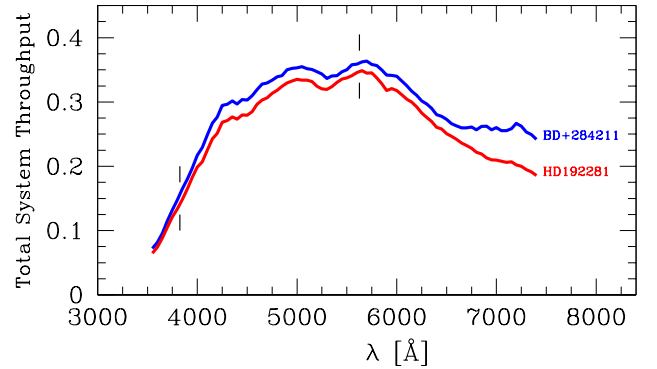


Figure 2. Total system throughput – telescope mirrors, spectrograph grating, optics, and CCD – measured from a hot (BD+284211, blue line) and cool (HD192281, red line) flux standard star on 2014 October 16. The overall shape reflects the blaze function of the 300 line mm^{-1} grating; second-order light contamination can be seen $>6500\text{ \AA}$ where the blue line diverges from the red line. Black lines mark the wavelengths plotted in Figure 3.

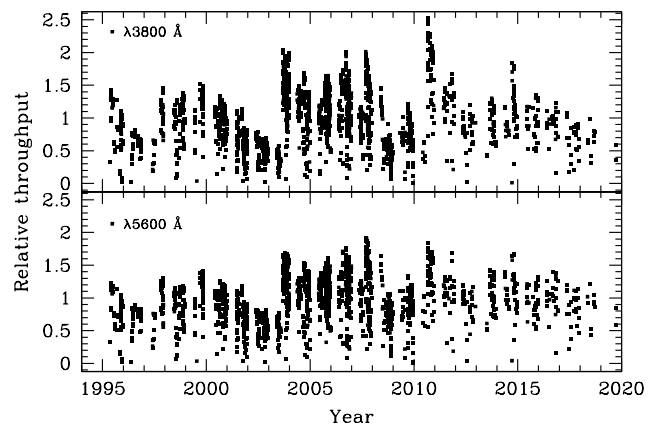


Figure 3. Relative throughput versus time, measured from the flux of BD+284211 at 3800 \AA (upper panel) and 5600 \AA (lower panel), normalized to the mean of 25 years of observations. The upper envelope of points reflects system throughput; low points are meaningless, due to bad pointing or non-photometric conditions. Jumps in throughput are seen when the primary mirror is re-aluminized or the optics are cleaned.

Notably, the relative throughput jumps up by a factor of 2 in the red and 4 in the blue when the primary mirror is re-aluminized (every 2 to 4 years) or the corrector optics are cleaned (at more irregular intervals).

3. OBSERVATIONS

We provide a brief summary of FAST operations to help users understand the spectra present in the public archive. We discuss the issue of flux calibration, and then quantify the precision and accuracy of the FAST wavelength calibration.

3.1. *Scheduling*

Observing time is allocated and scheduled on a trimester basis: January-April, May-August, and September-December. Approved FAST programs are assigned program numbers, stored in the FITS headers as PROGRAM, that identify which spectra belong to which observing program. A program which lasts more than one trimester keeps the same number. Principle investigator name or names are stored in the FITS headers as P.I., with periods. These provide two means of sorting spectra.

Principle investigators provide the target coordinates for their scientific programs, which are recorded in the FITS header as requested RA and DEC. Some programs target a single class of sources, such as a galaxy redshift program. Other programs classify unknown sources, or have target selection that shifts over time, and so accumulate a more diverse set of spectra under a single program number.

FAST observations are acquired in queue mode, not in classically scheduled nights. Queue scheduling has enabled P.I.s to run long-term monitoring programs as well as target-of-opportunity programs. Queue scheduling also enables observers at the telescope to optimize target selection and exposure times for the conditions of each night.

3.2. *Observing*

Historically, FAST was mounted on the telescope every month for a ~ 2 week observing run centered around new moon. Thus FAST observations are obtained with a nightly and a monthly cadence. The exception is August, when FLWO closes for maintenance during the worst of the Arizona monsoon weather.

Observers at the telescope follow a strict protocol. A complete set of FAST calibrations are obtained every night. Ten bias frames and five 15 minute dark frames are obtained in each spatial binning. Twenty-one flat-fields are obtained in each spectrograph configuration. All science exposures are immediately followed by a comparison lamp exposure for accurate wavelength calibration.

3.3. *Target Acquisition*

Observers have to visually identify targets on the slit-viewing guide camera, i.e. by matching star patterns to finding charts, and manually place targets on the spectrograph slit by eye. This process can be challenging because the FLWO 1.5m telescope pointing is poor, with an accuracy of about 2 arcmin over most of the sky. The telescope position recorded in the fits header (TRA, TDEC) thus differs from the requested position (RRA,

RDEC). This discrepancy is normal but uninformative. The values assigned to RA and DEC in the FITS headers are taken from the requested positions provided by the P.I.'s, and precessed to J2000 if necessary.

FLWO staff observers are very good at identifying targets. Cross-checks suggest that $>99.9\%$ of spectra are of the correct target. In rare cases, however, the wrong target may be observed. In other rare cases, the correct object is observed, but the data acquisition system records the wrong coordinate if the telescope was slewed during readout, or if the coordinates were stale from the telescope coming out of a shutdown situation. Other “incorrect” targets are actually real, such as candidate supernovae that turn out to be high proper motion stars superimposed on background galaxies. Outlier spectra should thus be treated with caution.

3.4. *Flux Calibration*

Every night, observers obtain spectra of red and blue stellar flux standards from [Massey et al. \(1988\)](#) in every spectrograph configuration used. The flux standards are labeled with FAST program #56 Spectrophotometric Standards. Spectra can be obtained in variable nonphotometric conditions, however. Thus, flux standards are best used for correcting the spectral continuum shape, and not for determining absolute flux calibration.

Flux calibration was never integrated into the FAST data reduction pipeline, however. The reason is that most FAST spectra have wavelength-dependent flux loss because the observations were made at a fixed position angle of 90° , not the parallactic angle. FAST is mounted on a mechanical rotator bearing and can be rotated to any position angle, but the process was time-consuming and rarely used. The major exceptions were FAST programs #2 Supernovae and #56 Spectrophotometric Standards, which set the position angle to the parallactic angle for their targets. The position angle value is stored in the FITS header as POSANGLE prior to 2002 November 12 and ROTANGLE after 2002 November 12.

An atmospheric dispersion corrector, installed during the 2010 August shutdown, now makes it possible to more accurately flux-calibrate FAST spectra. Second-order light still overlaps the red end of the spectrum, however (Figure 2).

Because flux calibration is unnecessary for measuring galaxy redshifts, flux calibration was deferred to the user. [Matheson et al. \(2008\)](#) describe how they combine red and blue standards to flux-calibrate FAST spectra for the supernova program.

3.5. *Wavelength Calibration*

All FAST spectra are wavelength-calibrated using helium-neon-argon comparison lamp exposures obtained

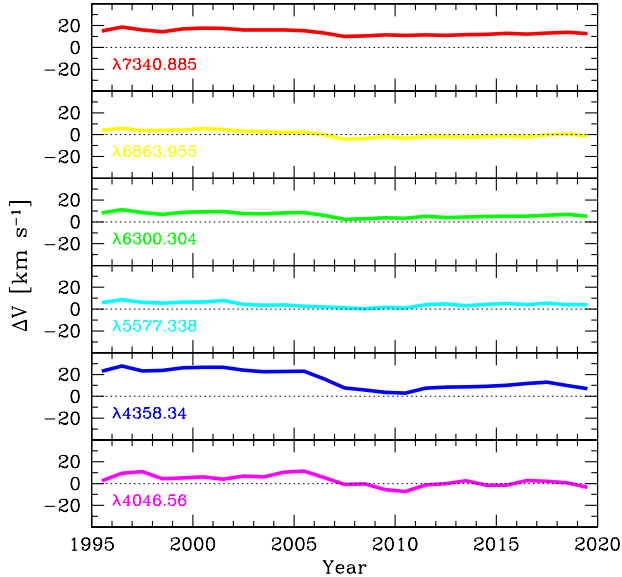


Figure 4. Weighted-mean velocities of night-sky emission lines relative to their rest-frame velocity (dotted line) versus year of observation. We conclude that FAST wavelength calibration is accurate at the 10 km s^{-1} level.

immediately after every science exposure. The only exception to this rule are time-series of short exposures, which can share a single comparison lamp exposure.

We test the precision of FAST’s wavelength calibration with the radial velocities of flux standard stars. The FAST archive contains over a thousand spectra of stars like Feige34, BD+284211, and HD84937. We find that a given flux standard exhibits an RMS dispersion of $\pm 32 \text{ km s}^{-1}$ with the 3.0 arcsec slit configuration, and $\pm 12 \text{ km s}^{-1}$ with the 1.5 arcsec slit configurations. Slit illumination effects likely explain the difference. Since typical seeing is around 1.5 arcsec, we consider $\pm 12 \text{ km s}^{-1}$ an empirical estimate of radial velocity precision.

Second, we test the accuracy of FAST’s wavelength calibration by measuring the radial velocity of night sky emission lines (see Table 3). The night sky uniformly illuminates the slit and is at rest with respect to the telescope. We measure velocity with the cross-correlation program EMSAO (Kurtz & Mink 1998) for 27,583 spectra obtained with the 300 line mm^{-1} grating and $>900 \text{ s}$ exposure times. We clip $>4\sigma$ outliers, because cosmic rays were not removed from the sky spectra, and compute weighted mean velocities by year for each line. We plot the results in Figure 4.

Figure 4 reveals both wavelength- and time-dependent trends. Prior to the FAST3 CCD upgrade in 2006 June, the night sky lines are systematically shifted in veloc-

Table 3. Weighted-Mean Velocity of Night-Sky Lines

Line	λ (\AA)	RV _{pre-2006.5} (km s^{-1})	RV _{post-2006.5} (km s^{-1})
HgI	4046.56	+7.1	−1.1
HgI	4358.34	+24.3	+7.5
HgI	5460.74	+22.8	+13.8
[OI]	5577.338	+5.5	+2.9
[OI]	6300.304	+8.3	+4.1
[OI]	6363.776	+7.4	+4.6
OH7-2Q1(1.5)	6863.955	+3.7	−2.4
OH8-3P1(3.5)	7340.885	+16.2	+11.4

ity from $+5 \text{ km s}^{-1}$ at $\lambda 5577 \text{ \AA}$ to about $+20 \text{ km s}^{-1}$ at the red and blue ends of the spectrum. We attribute the systematic offset to the difference in how the helium-neon-argon calibration lamp illuminates the spectrograph compared to the night sky. The accuracy improves after 2006 June, to a weighted mean over all lines of $+5.6 \pm 0.1 \text{ km s}^{-1}$. We conclude that the FAST wavelength calibration has an effective precision and accuracy at the 10 km s^{-1} level.

4. DATA REDUCTION PIPELINE

FAST spectra have been processed with essentially the identical IRAF-based data reduction pipeline (Tokarz & Roll 1997) since first light in 1994 January. In the first decade of operation, however, only data obtained with the “standard” DISPERSE=300, TILT-POS=590, APERTURE=3 configuration were processed. P.I.’s were expected to process the other $\sim 10,000$ spectra obtained in nonstandard configurations.

Beginning in 2006 June (with the FAST3 CCD upgrade), we updated the pipeline to work with all spectrograph configurations, and have processed every FAST observation. As of 2019 December 31, the SAO OIR Telescope Data Center has processed 156,899 of the 166,979 total science spectra acquired by FAST.

We process, archive, and distribute FAST data on a daily basis. Figure 5 illustrates the workflow. Each morning, a cron job automatically transfers raw data from Mt. Hopkins to a local archive at SAO. We use WCSTools (Mink 2002) to read the FITS headers, and Unix shell scripts to sort the data by spectrograph configuration. Data from each configuration is then run through the IRAF data reduction pipeline. The results are cataloged, archived, and distributed to the appropriate P.I.s. The final data products are linearized,

Table 4. Largest Programs in the Public Archive (2019 December 31)

N_{spectra}	N_{unique}^*	Prog. #	Program Title	P.I.
17019	103	56	Spectrophotometric Standards	All
11913	457	57	Velocity Standard	All
8132	1720	2	Supernovae	Kirshner
8071	95	6	AGN Monitoring	Wilkes
7622	6803	68	2MASS Redshift Survey	Huchra
6938	6400	64	Cluster Infall Regions	Geller
5764	5200	141	2MASS Redshift Survey	Falco
5301	4482	3	15R Redshift Survey	Geller
5013	1911	178	Low Mass White Dwarfs	Brown
4911	3302	1	CfA Redshift Survey	Huchra/Geller
4029	3472	112	Pre-Main Sequence Stars in Orion	Calvet
2936	2795	59	X-ray Groups	Mahdavi
2927	2449	157	IPHAS	Steeghs
2263	2	12	Symbiotic Stars	Kenyon
2128	1045	89	Ae/Be Stars	Calvet
2050	1413	60	CfA Redshift Survey Completion	Geller

* Defined as targets with unique OBJECT names separated by >10 arcsec, excluding twilight-sky spectra.

We perform cross-correlation with the package RVSAO described in detail by Kurtz & Mink (1998). Briefly, we subtract the continuum, apodize, and Fourier filter each spectrum. We then cross-correlate the full spectrum against a library of stellar and galaxy templates, rebinned onto a common log-wavelength scale. We estimate the velocity and velocity error from the peak and width of the cross-correlation peak following Tonry & Davis (1979).

We present the cross-correlation templates in Appendix B, and caution that some spectral types of objects – quasars, supernovae, M dwarfs, helium stars, continuum objects – have no valid template and/or can latch on to a bogus template. We use QPLOT to visually inspect and validate the velocity of each spectrum.

Figure 6 shows the example of NGC 4116 with its best-fit emission and absorption lines labeled. The QPLOT task allows us to remove cosmic rays, which can confuse emission line fits, and re-correlate if necessary. We then set the quality flag to approve (VELQUAL=“Q”) or disapprove (VELQUAL=“X”) the cross-correlation.

The full list of cross-correlation keywords is presented in Appendix C; the most important keywords for the user are VELOCITY, the best-fit radial velocity in km s^{-1} , CZXCERR, the velocity error in km s^{-1} , BEST-TEMP, the best-matching template, and CZXCR, the r statistic (analogous to signal to noise) of the fit. These

values are a guide to the nature of an object (BEST-TEMP, VELOCITY) and the quality of its spectrum (CZXCR, CZXCERR).

Scientists typically perform follow-up analysis optimized for their sources. Published velocities thus supersede the velocities recorded in our FITS headers.

4.2. Data Archiving and Distribution

Processed 1D and 2D spectra are normally distributed to P.I.s within one working day of acquisition, using a shell script that sends email notifications with download instructions. Both raw and processed files are archived for permanent storage. Files are stored first to a local RAID-array archive in Cambridge, MA, and are mirrored quarterly to an off-site Smithsonian computing facility in Herndon, VA. Copies are also retained at FLWO for several years, to ensure there is always a copy at multiple distinct sites.

Metadata used by the public archive are ingested and stored in a PostgreSQL database residing in Cambridge and on our cloud server that hosts the <http://oirsa.cfa.harvard.edu> public interface. The public archive is described next.

5. THE PUBLIC ARCHIVE

The CfA Optical Infrared Science Archive (OIRSA) was released by the SAO Telescope Data Center in early 2016. The goal was to make a complete set of *processed*

spectra, obtained from optical/infrared spectrographs on the CfA’s ground-based telescopes, available to the public.

OIRSA uses the German Astrophysical Virtual Observatory Data Center Helper Suite (DaCHS) (Demleitner et al. 2014), a publishing infrastructure for the Virtual Observatory. DaCHS exploits the open-source PostgreSQL object-relational database management system¹ with specific extensions to provide flexible data search and access mechanisms to astronomical data (Chilingarian et al. 2004). The DaCHS access mechanisms are built on top of an existing PostgreSQL database schema and operate on an SQL view created from joining several data tables. Our database schema implements our own proprietary data model, which we reuse with minor modifications across the public and private data archives for different instruments and also for operations of the Binospec (Fabricant et al. 2019) and MMIRS (McLeod et al. 2012) spectrographs at the 6.5-m MMT telescope.

DaCHS data access services for the OIRSA archive implement several International Virtual Observatory Alliance (IVOA) standards: (i) the Simple Spectral Access Protocol (Tody et al. 2012) providing access to one-dimensional extracted spectra; (ii) Observation Data Model Core Components, its Implementation in the Table Access Protocol (Tody et al. 2011) providing a more generic and flexible query interface to the metadata search including the cross-match via table upload; (iii) Registry Interfaces (Dower et al. 2018) that tell the Virtual Observatory about the existence of OIRSA data access services and make it discoverable in client applications such as TOPCAT (Taylor 2005).

The OIRSA archive debuted with over 290,000 processed 6.5 m MMT Hectospec spectra, homogeneously reduced with the latest data reduction pipeline and linked to published papers. The Hectospec archive is updated yearly and includes every spectrum older than 10 years old. Second to be added were over 250,000 single-order echelle spectra, each with wavelength coverage of 45 Å and spectral resolution of about 36,000 centered at 5187 Å. The echelle spectra were obtained with cross-dispersed echelle spectrographs using 2 x 936-pixel Reticon detectors on the FLWO 1.5-meter Tillinghast telescope, the 4.5 m-equivalent Multiple Mirror Telescope, and the 1.5-meter Wyeth telescope at Oak Ridge Observatory in Harvard, Massachusetts (Mink et al. 2019). The echelle spectra were primarily obtained for radial velocity studies of bright stars, and the uniformly pro-

cessed spectra provide a valuable resource in combination with Gaia proper motion and parallax measurements.

DaCHS provides a simple web-based query form, which allows one to search and download spectra in bulk and which actually queries TAP and SSAP services in the backend. For example, a list of up to 280 target positions along with search radii can be queried with the web form; OIRSA returns the resulting batch of spectra in a tarball file. Much larger queries can be made with Virtual Observatory tools like TopCat (Taylor 2005). Thanks to the implementation of IVOA standards, the OIRSA FAST Archive can be queried in a batch mode using scripts in several programming languages (Python, Shell, IDL, Java) using Application Programming Interface libraries.

6. RECOMMENDATIONS FOR USE

OIRSA currently contains 141,531 processed FAST spectra obtained between 1994 January and 2019 December. We have removed many of the completely failed observations, such as saturated spectra or spectra with zero counts. However, we have erred on the side of retaining everything else. The archive contains over 5,500 twilight sky spectra, for example, observations that can sometimes point at real objects although only twilight sky is visible.

A good rule of thumb is that spectra with CZXCR>3 are mostly reliable; spectra with CZXCR<3 are mostly noise. Fully 87.5% of the reduced FAST spectra have VELQUAL=Q and CZXCR>3, spectra that should be ready to use.

A generous search radius should be used if cross-matching the FAST archive by position. We record RA and DEC in epoch J2000, but the equinox on which the coordinates are based is unknown. Galaxy coordinates that come from photographic plates have ~10 arcsec coordinate uncertainties (Falco et al. 1999). Stellar coordinates that come from modern surveys like SDSS have <1 arcsec uncertainties but, unlike galaxies, can have significant proper motion.

A powerful approach for using FAST spectra is to start with published, well-defined surveys. Table 4 lists the largest programs in the public archive: all programs with >2000 spectra as of December 31, 2019. The median visual magnitude of targets in the FAST archive is around 15 mag; the faintest point sources are 18 mag.

6.1. Signature FAST Programs

Signature programs include the CfA Redshift Survey (Geller & Huchra 1989), Updated Zwicky Catalog (Falco et al. 1999), and the 2MASS Redshift Survey

¹ <https://www.postgresql.org/>

(Huchra et al. 2012). A number of the redshifts for those surveys were measured with FAST.

Redshift surveys made entirely with FAST observations include the 15R Redshift Survey (Carter et al. 2001), the Cluster and Infall Region Nearby Survey (Rines et al. 2003), and the X-ray emitting nearby galaxy groups program (Mahdavi & Geller 2004).

One of the largest programs is the CfA Supernova Program, which obtained over 8000 spectra for bright $V < 18$ mag supernovae over the past quarter century. The public archive contains the spectra but not the final reductions published by the CfA Supernova Program, so we refer the user to their papers (Matheson et al. 2008; Blondin et al. 2012; Hicken et al. 2017).

Other major holdings include Galactic plane surveys of young emission line stars (Hernández et al. 2005; Raddi et al. 2015), long-term monitoring programs of active galactic nuclei (Trichas et al. 2012) and of symbiotic star binaries (Kenyon & Garcia 2016; Cúneo et al. 2018), and time-series spectroscopy of low-mass white dwarf candidates (Brown et al. 2010). A few programs are missing from the archive because their spectra were obtained prior to 2006 in nonstandard configurations. The largest missing program is the Century Survey Galactic Halo Project (PROGRAM=122) that measured radial velocities for over 4,000 blue horizontal branch star candidates (Brown et al. 2008).

Selecting spectra by PROGRAM or P.I. does not guarantee a complete set, however. Thus, we provide tar files of spectra for some major programs on the public archive web page.

7. CONCLUSIONS

Our hope is that making reduced FAST spectra easily accessible will enable scientists to make good use of the spectra for decades to come. A surprising number of 16th magnitude galaxies in SDSS lack redshifts due to the fiber-positioning constraints of the SDSS spectrograph (Lazo et al. 2018), for example. Some of those galaxies are found in the FAST archive. Gaia likely provides parallax and proper motions for every star that FAST has ever observed, but most of the hot stars lack radial velocities, velocities that can be found in the FAST archive. We encourage users to explore the spectra collected with FAST over the past quarter century. The OIRSA will add processed spectra taken with other CfA instruments in future years.

The data in this paper were taken using the FAST spectrograph by a number of observers, the most prolific of whom were Perry Berlind (70,891 spectra), Mike Calkins (38,543 spectra), Jim Peters (4345 spectra), Ken Rines (3953 spectra), John Huchra (3762 spectra), Warren Brown (3759 spectra), and Lucas Macri (2957 spectra). I.C. is supported by the Telescope Data Center at SAO and also acknowledges the Russian Science Foundation grant 19-12-00281.

Facility: FLWO:1.5m

APPENDIX

A. GRATING TILT EQUATIONS

The following relations link grating tilt, set by the micrometer TILTPOS value, to the approximate central wavelength (CW) in units of Å. The 1200 line mm^{-1} grating has two equations because the micrometer must be used with a spacer to tilt the grating to blue wavelengths.

$$300 \text{ l mm}^{-1} \quad \text{CW} = 13.2 * \text{TILTPOS} - 2400 \text{ Å} \quad (\text{A1})$$

$$600 \text{ l mm}^{-1} \quad \text{CW} = 6.61 * \text{TILTPOS} + 1600 \text{ Å} \quad (\text{A2})$$

$$1200 \text{ l mm}^{-1} \quad \text{CW} = 3.29 * \text{TILTPOS} + 5200 \text{ Å} \quad (\text{A3})$$

$$\text{spacer} + 1200 \text{ l mm}^{-1} \quad \text{CW} = 3.51 * \text{TILTPOS} + 3850 \text{ Å} \quad (\text{A4})$$

B. FAST CROSS-CORRELATION TEMPLATES

Our quality control check uses one of two sets of cross-correlation templates listed in Table 5, a total of 37 spectra assembled at different times for different programs. Most of the templates were made empirically, by combining high signal-to-noise observations of objects of known velocity using the IRAF RVSAO SUMSPEC task (Mink 2013) or using our IRAF singular value decomposition task SVDFIT (Kurtz & Mink 2000) when a large number of spectra were combined. Emission line templates were generated by the LINESPEC task in the RVSAO package (Kurtz & Mink 1998).

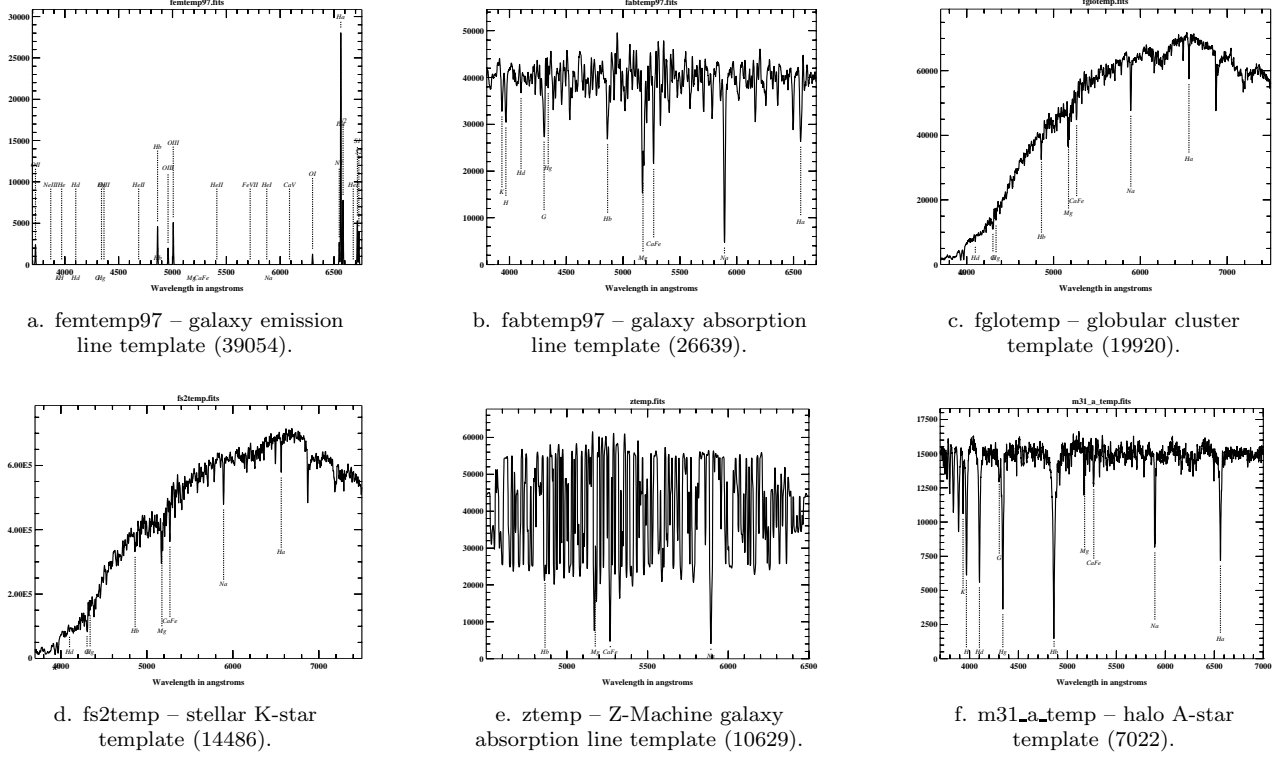


Figure 7. Six most-used cross-correlation templates in the FAST reduced spectra archive (number as of Dec 31, 2019).

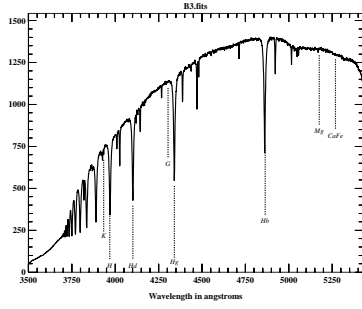
All of the cross-correlation templates are distributed with the RVSAO package (Kurtz & Mink 1999). Characteristics of all of these templates are given in Table 5.

Figure 7 plots the six most commonly used templates in the FAST archive. These templates are primarily intended to measure galaxy redshifts from spectra obtained with the standard DISPERSE=300, TILTPOS=600, APERTURE=3 setup. These six templates account for 75% of the cross-correlation velocities in the FAST reduced spectra archive.

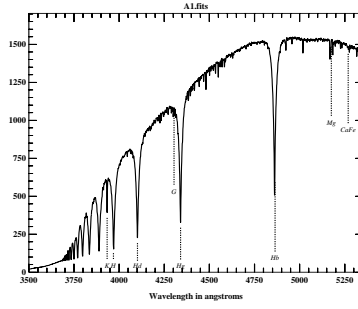
fglotemp and fs2temp were made in 1994 and 1995, respectively, from FAST globular cluster spectra obtained with the first two CCD detectors. The K-type spectra were thought to provide a good match for absorption line galaxies. femtemp97 and fabtemp97 were made in 1997 to better fit galaxy emission and absorption line spectra, respectively. ztemp was made from absorption line galaxies observed with the old Z-Machine spectrograph. m31_a_temp was made in 2002 from halo A-type stars observed with the MMT Hectospec spectrograph (from a program that targeted M31). The A-type template provides a better match to flux standard stars and white dwarfs.

Figure 8 plots selected templates from a series of stellar spectral-type templates, constructed in 2002 from the spectra of bright stars observed with the DISPERSE=600, TILTPOS=445, APERTURE=2.0 setup. A full series of spectral-type templates was made for PROGRAM=122 (Brown et al. 2003) and are distributed with the RVSAO package; however, the spectra used to make the templates were obtained before 2006 and do not appear in the FAST reduced spectra archive. The stellar templates in Figure 8 account for 4% of the cross-correlation velocities in the FAST reduced spectra archive.

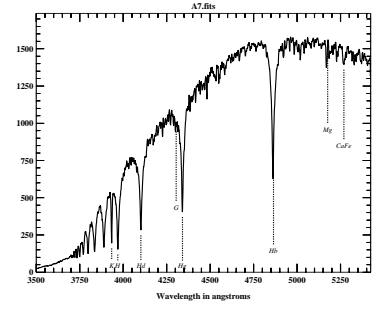
We remind the reader that cross-correlation velocities are accurate only if the template matches the target. We have no template for certain spectral classes, such as helium stars, M dwarfs, quasars, and supernovae. Thus, we urge users to analyze FAST spectra with cross-correlation templates optimized for their actual needs.



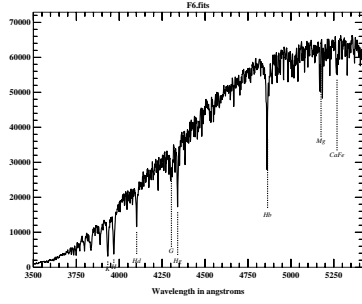
a. B3 template.



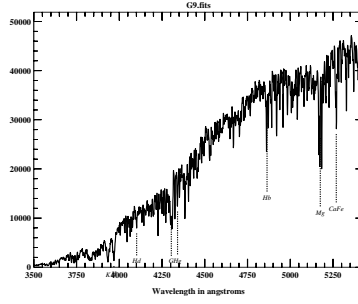
b. A1 template.



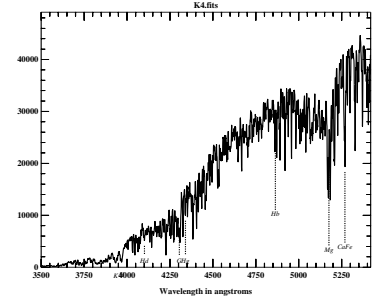
c. A7 template.



d. F6 template.



e. G9 template.



f. K4 template.

Figure 8. Selected stellar templates for the DISPERSE=600 TILT=445 FAST program.

Table 5. Cross-Correlation Templates

Template	Nbest	First Night	Last Night	Npix	Range (Å)	Res.(Å)	Continuum	Comments
Templates for the standard DISPERSE=300 TILT=600 configuration								
eatemp	1106	1994 Jun 05	2019 Nov 22	4505	2979-7000	6.0	Subtracted	Elliptical galaxy+A-star Hectospec
eltemp	947	1994 Jun 14	2019 Nov 22	4505	2979-7331	6.0	Instrumental	Elliptical galaxy Hectospec
emtemp	7559	1994 Jan 11	2019 Dec 22	4096	3500-7500	6.0	Zero	Galaxy emission lines synthesized
f86btemp	2889	1994 Jul 03	1995 Jul 31	1850	3690-6402	7.2	Instrumental	NGC 4486b galaxy 5 FAST
fabtemp97	26638	1994 Jun 05	2019 Dec 21	2000	3800-6700	7.2	Divided	Absorption line galaxy
femtemp	645	1994 Jun 05	2019 Dec 22	20001	3000-8000	8.0	Zero	Galaxy emission lines
femtemp97	39054	1994 Jun 05	2019 Dec 22	10001	3000-8000	6.0	Zero	11 Galaxy emission lines
fglotemp	19920	1994 Jan 11	2019-12-22	4096	3700-7500	7.2	Instrumental	M31 cluster 225-280 15 FAST
fm32temp	6420	1994 Jan 11	2019 Dec 21	4096	3700-7500	7.2	Instrumental	M32 cluster stars 14 FAST
fn4486btemp	291	1994 Feb 02	1996 Jan 23	4096	3700-7500	7.2	Instrumental	NGC 4486b 23 FAST
fn5548temp	116	1994 Feb 02	1996 Jan 23	4096	3700-7300	7.2	Instrumental	Active galaxy NGC 5548 39 FAST
fn7331temp	6723	1994 Jan 11	2019 Dec 22	4096	3700-7500	7.2	Instrumental	NGC 7331 galaxy 16 FAST
fs2temp	14486	1994 Jan 11	2019 Dec 21	4096	3700-7500	7.2	Instrumental	Star AGK2p4392 53 FAST
fztemp97	26	1997 Jul 30	1997 Aug 03	2000	3800-6700	7.2	Divided	Absorption galaxies 1,979 FAST
m31_a_temp	7021	1994 Jun 05	2019 Dec 22	4000	3700-7000	6.0	Divided	A stars 39 Hectospec
m31_f_temp	1421	1994 Jun 09	2019 Nov 22	4000	3700-7000	6.0	Divided	F stars 72 Hectospec
m31_k_temp	1362	1994 Jun 05	2019 Dec 21	4000	3700-7000	6.0	Divided	K stars 69 Hectospec
skytemp	18	1998 Nov 16	2014 Apr 30	6002	4000-7000	6.0	Zero	10 Night-sky emission lines
sptemp	2010	1994 Jun 05	2019 Nov 23	4505	2984-7379	6.0	Instrumental	Spiral galaxy Hectospec
stemp	1231	1994 Jul 03	1995 Jul 31	2048	4500-6500	4.8	Divided	Composite star Z-Machine
ztemp	10602	1994 Jan 11	2019 Dec 22	2048	4500-6500	4.8	Divided	Composite galaxy Z-machine
Stellar templates for the DISPERSE=600 TILT=445 configuration								
A1	840	2006 Sep 17	2019 Sep 30	2679	3500-5352	2.3	Instrumental	A1 star combined FAST spectra
A4	2361	2006 Sep 15	2019 Sep 30	2679	3500-5423	2.3	Instrumental	A4 star combined FAST spectra
A7	241	2006 Sep 17	2019 Sep 29	2683	3500-5423	2.3	Instrumental	A7 star combined FAST spectra
B3	442	2002-04-03	2019 Sep 29	2679	3500-5427	2.3	Instrumental	B3 star combined FAST spectra
B7	615	2006 Sep 15	2019 Sep 29	2679	3500-5418	2.3	Instrumental	B7 star combined FAST spectra
B9	1058	2006 Sep 15	2019 Sep 30	2682	3500-5419	2.3	Instrumental	B9 star combined FAST spectra
F2	99	2006 Sep 16	2019 Jun 05	2679	3500-5423	2.3	Instrumental	F2 star combined FAST spectra
F4	382	2008 Apr 15	2019 Jul 02	2679	3500-5420	2.3	Instrumental	F4 star combined FAST spectra
F6	88	2010 Apr 10	2019 Mar 14	2679	3500-5419	2.3	Instrumental	F6 star combined FAST spectra
F8	44	2010 May 08	2019 Jul 02	2679	3500-5423	2.3	Instrumental	F8 star combined FAST spectra
F9	23	2010 May 09	2019 Jun 04	2679	3500-5418	2.3	Instrumental	F9 star combined FAST spectra
G2	33	2010 May 09	2019 Jun 05	2684	3500-5419	2.3	Instrumental	G2 star combined FAST spectra
G6	17	2006 Sep 28	2019 Sep 30	2679	3500-5419	2.3	Instrumental	G6 star combined FAST spectra
G9	63	2010 Sep 09	2019 Sep 30	2679	3500-5426	2.3	Instrumental	G9 star combined FAST spectra
K1	26	2010 Dec 01	2019 Sep 29	2679	3500-5418	2.3	Instrumental	K1 star combined FAST spectra
K4	80	2006 Dec 21	2019 Sep 29	2679	3500-5418	2.3	Instrumental	K4 star combined FAST spectra

C. FITS HEADER PARAMETERS

The following tables document the keywords in the reduced FITS file headers. Table 6 defines the keywords created by the telescope data acquisition system. Table 7 defines the keywords added by the data reduction pipeline. Table 8 defines the keywords added by the cross-correlation task, XCSAO, and the confirmation task, QPLOT (Tokarz & Roll 1997; Kurtz & Mink 1998). The overall listing reflects the order in which the keywords normally appear in the FITS file headers.

Table 6. FITS Image Header Keywords Generated by the Telescope Data Acquisition System

Keyword	Example Value	Description or Long Example Value
SIMPLE	T	Fits standard file
BITPIX	-32	Bits per pixel -32=4-byte floating point
NAXIS	2	Number of axes
NAXIS1	2681	Dispersion axis length in pixels
NAXIS2	1	Number of objects in file
NAXIS3	4	Spectra in file: 1=spectrum 2=sky+spectrum 3=sky 4=variance
EXTEND	F	File has no extensions
ORIGIN		NOAO-IRAF FITS Image Kernel July 2003
DATE	2013-03-18T19:29:11	Date this FITS file was generated
IRAF-TLM	2013-03-18T19:42:34	Time of last modification
OBJECT	NGC4116	Object name
NAMPS	1	Number of amplifiers read out for original 2-D spectrum
DATE-OBS	2013-03-18	UT YYYY-MM-DD at start of exposure
RA	12:07:36.81	Right Ascension
DEC	+02:41:32.3	Declination
EPOCH	2000	Equinox of coordinates
POSANGLE	90	Spectrograph position angle [prior to November 12, 2002]
ROTANGLE	90	Spectrograph position angle [after November 12, 2002]
FASTFOC	1350	FAST spectrograph focus setting
AIRMASS	1.18	Airmass
RRA	12:07:42.1	Requested Right Ascension
RDEC	+02:41:32.3	Requested Declination
REPOCH	2000	Requested Equinox
TRA	12:07:42.1	Telescope Right Ascension
TDEC	+02:44:03.3	Telescope Declination
TEPOCH	2000	Telescope coordinate equinox
ST	11:06:11	Sidereal time hh:mm:ss at start of exposure
HA	-01:02:12	Hour Angle hh:mm:ss at start of exposure
DOME	117	Dome azimuth angle in degrees
UT	06:31:30	UT hh:mm:ss at start of exposure
UTEND	07:01:30	UT HH:MM:SS at end of exposure
ST	'09:27:23'	Telescope Sidereal Time at end of exposure
MJD	56365.282292	Modified Julian Date at exposure midtime

Table 6 continued

Table 6 (*continued*)

Keyword	Example Value	Description or Long Example Value
GJDN	2456365.782292	Geocentric Julian Date at exposure midtime
HJDN	2453795.75925	Heliocentric Julian Date at exposure midtime
SITENAME	'flwo1'	Observatory name = FLWO 1.5m
SITELONG	'+110:52:39.0'	Observatory longitude in degrees west of 0 ddd:mm:ss
SITELAT	'+31:40:51.4'	Observatory latitude in degrees dd:mm:ss
SITELEV	2320.0	Observatory elevation in meters
DETECTOR	FAST3	detector identifier
CCDSERIA	STA520A SN4377	Chip ID
INSTRUME	FAST	instrument name
DISKDIR	/data/fast/2013.0313	Original raw directory with local date yyyy.mmdd
DISKFILE	81	File number in original raw directory
TELESCOP	'TILLINGHAST'	1.5 meter (60 inch) telescope
EXPTIME	1800.000	Integration time in seconds
DARKTIME	1800.000	Total elapsed time in seconds
IMAGETYP	OBJECT	IRAF spectrum type (object flat comp bias dark)
CCDSUM	1 2	Binning of raw image X (dispersion) and Y (cross-dispersion) axes
BIN	2	Binning of cross-dispersion axis
LTM1_1	1.0000000	IRAF pixel/pixel in X
LTM2_2	1.	IRAF pixel/pixel in Y
CCDSEC	[35:2715,1:161]	Actual detector image limits
GAIN	0.8000000	Read gain
RDNOISE	4.4000000	Read noise
OBSERVER	Brown	Telescope observer
P.I.	Zezas	Program principle investigator
PROGRAM		199 Optical nuclear spectroscopy of nearby galaxies'
APERTURE	3.0	Slit width on the sky in arcseconds
DISPERSE	300	Grating lines/mm
TILTPOS	600	Grating tilt toward blue i600 or red i600
COMMENT		Observer: Brown
COMMENT		P.I.: Zezas
COMMENT		Program: 199 nearby galaxies nuclear spectroscopy
COMMENT		Seeing: 1-2"
COMMENT		Aperture: 3"
COMMENT		Disperse: 300
COMMENT		Tiltpos: 600
COMMENT		Focus: 1350

Table 7. FITS Image Header Keywords Generated by the IRAF Data Reduction Pipeline

Keyword	Example Value	Description or Long Example Value
RFN	20130313.0081	Observation sequence = yyyyymmdd.nnnn
WCSDIM	3	Number of world coordinate system dimensions
WAT0_001	system=equispec	IRAF multispec format
WAT1_001		wtype=linear label=Wavelength units=angstroms
WAT2_001	wtype=linear	Cross-dispersion axis
TRIM		Mar 18 15:12 Trim data section is [35:2715,1:161]
OVERSCAN		Mar 18 15:12 Overscan section is [2:30,1:161] with mean=716.1741
ZEROCOR		Mar 18 15:12 Zero level correction image is zero
CCDMEAN	155.4683	Mean value of pixels in CCD image
CCDMEANT	1048086765	Number of counts in CCD image
CCDPROC		Mar 18 15:12 CCD processing done
FLATCOR		Mar 18 15:12 Flat-field image is norm with scale = 1
DCLOG1	Transform	Wavelength is transformed from dispersion to linear
DC-FLAG	0	Wavelength is linear, not log
CTYPE1	LINEAR	Dispersion axis is linear
CTYPE2	LINEAR	Cross-dispersion axis is linear
CRVAL1	3478.38037109375	Wavelength at center of reference pixel
CRPIX1	1.	Number of reference pixel in 1D spectrum first is 1
CD1_1	1.47133255004883	Wavelength per pixel
CD2_2	1.	Spectra per pixel
BANDID1		spectrum - background fit, weights variance, clean yes
BANDID2		raw - background fit, weights none, clean no
BANDID3		background - background fit
BANDID4		sigma - background fit, weights variance, clean yes
APNUM1	1 1 64.00 119.00	IRAF APALL extraction info
CTYPE3	LINEAR	Band spectra
CD3_3	1.	Band spectra per cross-dispersion pixel
LTM3_3	1.	IRAF pixel/pixel in BAND
WAT3_001	wtype=linear	One band spectrum per cross-dispersion pixel
FINDOBJ	85:92	Cross-dispersion pixel range for object extraction
FINDBACK	65:80,96:111	Cross-dispersion pixel ranges for background extraction

Table 8. FITS Image Header Keywords Generated by the XCSAO Radial Velocity Program

Keyword	Example Value	Description or Long Example Value
VELOCITY	1265.35069460358	Velocity in km/sec =cz from emission line
Z	0.00422075500422317	Velocity as z
CZERR	300.	Velocity error in km/sec set from emission line
ZERR	8.83416159802586E-6	Velocity error in km/sec

Table 8 continued

Table 8 (*continued*)

Keyword	Example Value	Description or Long Example Value
VELQUAL	Q	Velocity quality Q=good ?=questionable X=bad
BCV	4.2293119430542	Solar System barycentric velocity correction
CZXC	1289.70966527454	Cross-correlation velocity = cz
ZXC	0.00430200777295808	Cross-correlation z
CZXCERR	2.64841539087617	Cross-correlation error
CZXCR	51.4057371762259	Cross-correlation R-value
BESTTEMP	femtemp97.fits	Best cross-correlation template
CZPARAMS	13 4096 1 5 20 250 500 0.05	No.temps xcor: bins zeropad filterx4 bellwindow
COMMENT		rvsao.xcsao results for each template:
COMMENT		file name, cross-correlation velocity, error, R-value
COMMENT		correlation peak height (0-1) and width (km/sec)
COMMENT		velocity relative to template, template BCV
COMMENT		template em. chopped, template filtered
XCTEMP1		fabtemp97.fits 1317.375 34.757 6.7242 0.475 350.109 1316.788 0.000
XCTEMP2		ztemp.fits 1304.660 19.003 8.48857 0.469 237.782 1300.509 0.000 yes
XCTEMP3		femtemp97.fits 1289.710 2.648 51.4057 0.877 184.699 1285.354 0.000 n
XCTEMP4		fs2temp.fits 1281.685 28.899 6.66855 0.463 291.868 1277.337 0.000 ye
XCTEMP5		fglotemp.fits 1294.446 31.103 6.84486 0.458 319.406 1291.380 0.000 y
XCTEMP6		fm32temp.fits 1295.454 32.659 6.87543 0.462 336.430 1292.184 0.000 y
XCTEMP7		fn7331temp.fits 1262.144 48.538 6.40995 0.449 463.554 1257.691 0.000
XCTEMP8		eatemp.fits 1328.693 142.354 1.38256 0.098 495.571 1321.587 0.000 no
XCTEMP9		eltemp.fits 99085.439 292.865 1.71597 0.118 1093.522 99079.649 0.000
XCTEMP10		sptemp.fits 1304.153 6.535 23.2321 0.819 210.281 1271.864 -28.010 no
XCTEMP11		m31_a_temp.fits 100184.771 379.495 1.10537 0.080 1304.335 37205.074
XCTEMP12		m31_f_temp.fits 99610.749 148.512 1.59509 0.100 497.927 15643.079 0.
XCTEMP13		m31_k_temp.fits 77365.998 123.226 1.73377 0.124 618.769 86365.812 0.
XCSAO		rvsao.xcsao 2.8.2 18-Mar-2013 15:34 CZXC = 1289.71 R = 51.41
VELSET		Velocity from 6730.815A S2 emission line
QPLOT		rvsao.xcsao 2.8.2 18-Mar-2013 15:43 VELOCITY = 1265.35 Q = Q

REFERENCES

- Blondin, S., Matheson, T., Kirshner, R. P., et al. 2012, *AJ*, 143, 126
- Brown, W. R., Allende Prieto, C., Beers, T. C., et al. 2003, *AJ*, 126, 1362
- Brown, W. R., Beers, T. C., Wilhelm, R., et al. 2008, *AJ*, 135, 564
- Brown, W. R., Kilic, M., Allende Prieto, C., & Kenyon, S. J. 2010, *ApJ*, 723, 1072
- Carter, B. J., Fabricant, D. G., Geller, M. J., Kurtz, M. J., & McLean, B. 2001, *ApJ*, 559, 606
- Chilingarian, I., Bartunov, O., Richter, J., & Sigaev, T. 2004, in *Astronomical Society of the Pacific Conference Series*, Vol. 314, *Astronomical Data Analysis Software and Systems (ADASS) XIII*, ed. F. Ochsenbein, M. G. Allen, & D. Egret, 225
- Cúneo, V. A., Kenyon, S. J., Gómez, M. N., et al. 2018, *MNRAS*, 479, 2728
- Demleitner, M., Neves, M. C., Rothmaier, F., & Wambsganss, J. 2014, *Astronomy and Computing*, 7, 27
- Dower, T., Demleitner, M., Benson, K., et al. 2018, *Registry Interfaces Version 1.1, IVOA Recommendation 23 July 2018*, , doi:10.5479/ADS/bib/2018ivoa.spec.0723D
- Fabricant, D., Cheimets, P., Caldwell, N., & Geary, J. 1998, *PASP*, 110, 79
- Fabricant, D., Fata, R., Epps, H., et al. 2019, *PASP*, 131, 075004
- Falco, E. E., Kurtz, M. J., Geller, M. J., et al. 1999, *PASP*, 111, 438
- Geller, M. J., & Huchra, J. P. 1989, *Science*, 246, 897
- Hernández, J., Calvet, N., Hartmann, L., et al. 2005, *AJ*, 129, 856
- Hicken, M., Friedman, A. S., Blondin, S., et al. 2017, *ApJS*, 233, 6
- Huchra, J. P., Macri, L. M., Masters, K. L., et al. 2012, *ApJS*, 199, 26
- Kenyon, S. J., & Garcia, M. R. 2016, *AJ*, 152, 1
- Kurtz, M. J., & Mink, D. J. 1998, *PASP*, 110, 934
- . 2000, *ApJL*, 533, L183
- Kurtz, M. J., & Mink, J. 1999, *RVSAO 2.0: Digital Redshifts and Radial Velocities*, *Astrophysics Source Code Library*, , ascl:9912.003
- Lazo, B., Zahid, H. J., Sohn, J., & Geller, M. J. 2018, *rnaas*, 2, 234
- Mahdavi, A., & Geller, M. J. 2004, *ApJ*, 607, 202
- Massey, P., Strobel, K., Barnes, J. V., & Anderson, E. 1988, *ApJ*, 328, 315
- Matheson, T., Kirshner, R. P., Challis, P., et al. 2008, *AJ*, 135, 1598
- McLeod, B., Fabricant, D., Nystrom, G., et al. 2012, *PASP*, 124, 1318
- Mink, D. J. 2002, in *Astronomical Data Analysis Software and Systems XI*, Vol. 281, 169
- Mink, J. 2013, in *Astronomical Society of the Pacific Conference Series*, Vol. 475, *Astronomical Data Analysis Software and Systems XXII*, ed. D. N. Friedel, 291
- Mink, J., Rhee, J., & Latham, D. W. 2019, in *Astronomical Society of the Pacific Conference Series*, Vol. 521, *Astronomical Data Analysis Software and Systems XXVI*, ed. M. Molinaro, K. Shortridge, & F. Pasian, 132
- Raddi, R., Drew, J. E., Steeghs, D., et al. 2015, *MNRAS*, 446, 274
- Rines, K., Geller, M. J., Kurtz, M. J., & Diaferio, A. 2003, *AJ*, 126, 2152
- Taylor, M. B. 2005, in *Astronomical Society of the Pacific Conference Series*, Vol. 347, *Astronomical Data Analysis Software and Systems XIV*, ed. P. Shopbell, M. Britton, & R. Ebert, 29
- Tody, D., Micol, A., Durand, D., et al. 2011, *Observation Data Model Core Components, its Implementation in the Table Access Protocol Version 1.0, IVOA Recommendation 28 October 2011*, , doi:10.5479/ADS/bib/2011ivoa.spec.1028T
- Tody, D., Dolensky, M., McDowell, J., et al. 2012, *Simple Spectral Access Protocol Version 1.1, IVOA Recommendation 10 February 2012*, , doi:10.5479/ADS/bib/2012ivoa.spec.0210T
- Tokarz, S. P., & Roll, J. 1997, in *Astronomical Society of the Pacific Conference Series*, Vol. 125, *Astronomical Data Analysis Software and Systems VI*, ed. G. Hunt & H. Payne, 140
- Tonry, J., & Davis, M. 1979, *AJ*, 84, 1511
- Trichas, M., Green, P. J., Silverman, J. D., et al. 2012, *ApJS*, 200, 17